In-silico Analysis of In-stent Restenosis Prediction of Stented Renal Artery

Nurin Tihani Nazemi[1], Muhammad Faiz Md Shakhih[1], Mohamad Ikhwan Kori[1,5], Rudiyanto Philman Jong[2,3], Kahar Osman[2,4,5], Ishkrizat Taib[6]*

[1]Department of Biomedical Engineering and Health Sciences, Faculty of Electrical Engineering, Universiti Teknologi Malaysia, Skudai 81310, Johor, MALAYSIA
[2]Faculty of Mechanical Engineering, Universiti Teknologi Malaysia, Skudai 81310, Johor, MALAYSIA
[3]Department of Mechanical and Manufacturing Engineering, Faculty of Engineering, Universiti Malaysia Sarawak, Kota Samarahan 94300, Sarawak, MALAYSIA
[4]IJN-UTM Cardiovascular Engineering Center, Universiti Teknologi Malaysia, Skudai 81310, Johor, MALAYSIA
[5]Computational Fluid Mechanics Research Group, Faculty of Mechanical Engineering, Universiti Teknologi Malaysia, Skudai 81310, Johor, MALAYSIA
[6]Flow Analysis, Simulation, and Turbulence Research Group (FASTREG), Faculty of Mechanical Engineering and Manufacturing, Universiti Tun Hussein Onn Malaysia, Parit Raja, Batu Pahat, 86400 Johor, MALAYSIA
[*]mohamadikhwan@utm.my

ABSTRACT

In-stent restenosis (ISR) is a common complication after renal artery stenting, and stent design may influence the formation of ISR. This study aims to predict the effect of stent design on the risk of ISR formation after renal artery stenting. Using computer-aided design, a simplified renal artery model was modelled and later assembled with stents similar to commercial stents. Computational Fluid Mechanics (CFD) analysis was employed to simulate the blood flow in these stented models. Stent 1 exhibited superior hemodynamic performance with minimal low Wall Shear Stress (WSS) exposure in the stented region. Additionally, the study found that the thinnest Stent 1 was the most effective in reducing the risk of ISR formation. Thus, stent strut configuration with large

ISSN 1823-5514, eISSN 2550-164X
Received for review: 2024-01-01
Accepted for publication: 2024-04-25
Published: 2024-11-15

https://doi.org/10.24191/jmeche.v13i1.3754

spacing may reduce ISR risk, with the thinnest Stent 1 design showed promising performance in mitigating ISR. Hence, it is worth further investigation.

Keywords: *Renal Artery; In-Stent Restenosis; Computational Fluid Mechanics*

Introduction

Stenosis of the renal artery is caused by two major factors which are atherosclerosis or Fibromuscular Dysplasia (FMD) of the renal artery [1]. In renovascular disease, atherosclerosis is often reported, which causes the obstruction of blood flow that eventually leads to arterial stenosis [2]-[3]. Atherosclerotic Renal Artery Stenosis (ARAS) is often diagnosed in older patients due to systemic atherosclerosis and atherosclerotic changes present in the abdominal aorta [1], [4]. Stents were introduced to overcome the stenosis problem that behaves as a scaffold to maintain the lumen size [5], lessening blood flow restriction through it.

Previous studies in [6] and [7] found that around 30% occurrence of in-stent restenosis in patients who received stent treatment for their arterial stenosis. The modification of local hemodynamics properties due to stent insertion at the arterial wall was one of the causes of the restenosis occurrence [8]. The endothelial lining of the arterial lumen becomes damaged at the site of stent placement hence causing platelet accumulation as it is attracted to the injury site [5]. Hence, increasing the risk of in-stent restenosis.

Computational Fluid Dynamics (CFD) is a reliable tool for predicting and visualizing hydrodynamic and transport properties [9]. Hence, CFD can be used to simulate blood flow patterns and show areas of low wall shear stress [10], which have been associated with restenosis occurrence. CFD has also been utilized for in-silico studies for renal artery hemodynamics for patients with Renal Artery Stenosis (RAS) [11] with reconstructed patient-specific data from CT-scan images as the model [12]. It was supported by the findings that physiological Wall Shear Stress (WSS) affects endothelial function therefore instigating atherosclerosis which is also associated with ISR formation after stenting [13].

This paper contributes to the investigation of In-Stent Restenosis (ISR) which is a part of developing the most effective strategies for preventing and treating ISR. With that, it is crucial to find a suitable stent design for decreasing the rate of ISR. The aim of this paper is to predict and compare the occurrence of ISR formation in renal artery model stented with current commercial stents by CFD analysis and determining the stent parameters accountable. It is hoped that this project will benefit medical practitioners, especially doctors, and

surgeons, in the prognosis of treatment for patients with renal artery stenosis to minimize the possibility of ISR formation after stent implantation.

Methodology

Geometry

A simplified renal artery, shown in Figure 1 and Figure 2 was modeled using SOLIDWORKS and was used for the simulations. The dimensions of the simplified renal artery are based on the studies made by Mohammed et al. [14] and Stojadinovic et al. [15]. The renal artery diameter was set to 6 mm with the abdominal aorta at 15 mm in diameter [15]. The angle of both The Right Renal Artery (RRA) and Left Renal Artery (LRA) with respect to the abdominal aorta was set to 64.1º and 67.3º, respectively [15].

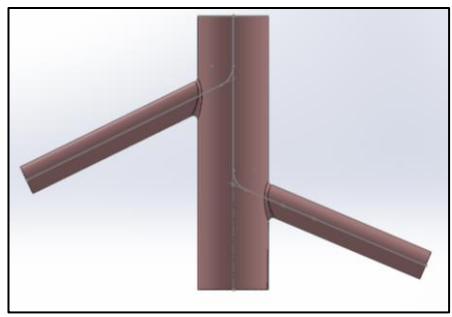

Figure 1: Simplified renal artery model

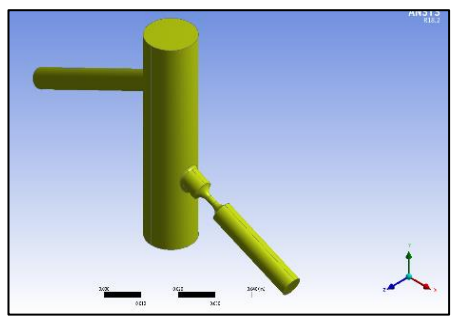

Figure 2: Renal artery model with 70% occlusion

The renal artery model was later assembled with 7 types of stents similar to commercial stents at the LRA region as explained by Taib et al. [16]. The

stents selected are shown in Figure 3. All the stent design parameters are shown in Table 1. Once the best stent design configuration is found, the thickness of the stent is modified from the original thickness, which is 0.15 mm and 0.25 mm.

Table 1: Stent design parameters

Parameters	Value (mm)
Length	8.0
Diameter	6.0
Thickness	0.2

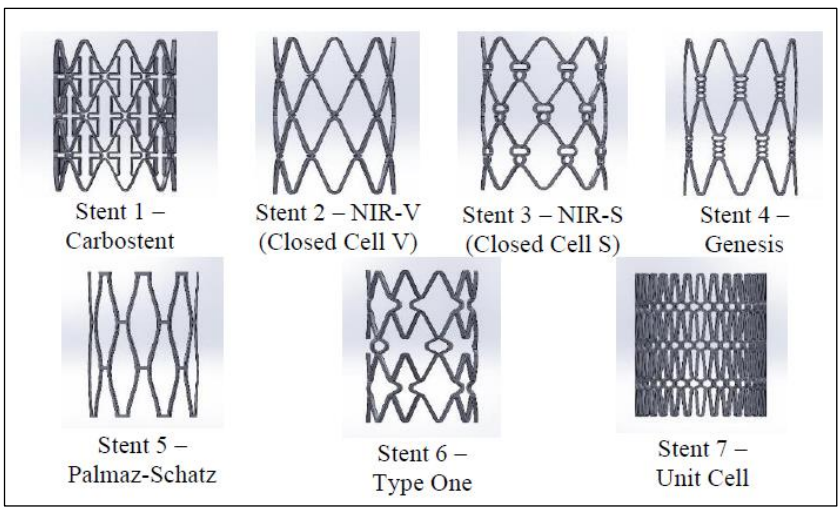

Figure 3: Selected stent designs for evaluation in this study [17]

Computational fluid dynamics modelling and simulation

In this study, the blood is defined to be a Newtonian fluid due to the inlet at the abdominal aorta is sufficiently large for the assumption to be valid. The blood is assumed to be incompressible with a density of 1050 kg/m^3 and viscosity of 0.00345 Pa.s [17]. The flow is governed by the Navier-Stokes equations (Equation (1) and Equation (2)):

$$\nabla \cdot u = 0 \tag{1}$$

$$\rho\left(\frac{\partial(\rho u)}{\partial t} + u \cdot \nabla - f\right) + \nabla p - \mu \nabla u = 0 \tag{2}$$

where u denotes the flow vector, ρ is the fluid density, p is the pressure and μ is the viscosity of the fluid. The model chosen for the simulation is the turbulence model to observe the complex blood flow, which in nature is susceptible to flow disturbance.

Figure 4 illustrates the boundary assigned to the stented renal artery model. The inlet is set at the proximal of the abdominal aorta and the outlets are set at the distal of the abdominal aorta, LRA, and RRA. The wall of the model is set to be rigid with no-slip condition [11]-[12], [18]. A steady inlet flow is defined at 0.2 m/s [19]-[20] at the descending aorta, with the outlet boundaries set to be 1 atm for free flow condition at the renal artery.

ANSYS Fluent is used to perform the simulations with the k-ω turbulence model was selected due to its k-omega model its suitability for near the wall flow region, where an adverse pressure gradient is developed [21]-[22].

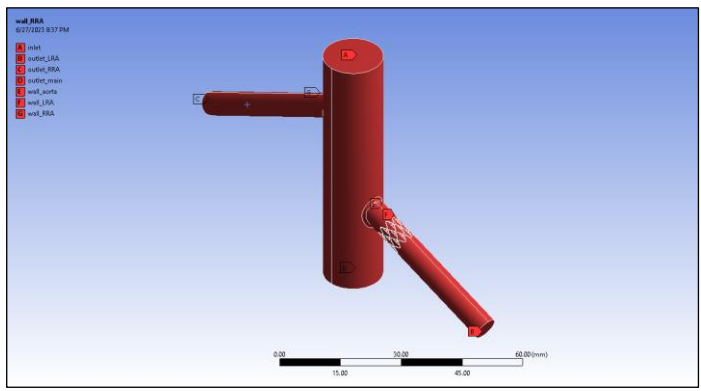

Figure 4: Assigned boundaries for stented renal artery model

Figure 5 shows the grid independence test results performed to determine the optimum mesh configuration for the simulation. A mesh face size of 0.75 mm with approximately 1.5 million nodes was selected for the simulation as the results indicated no significant difference with further improvement of mesh size and quantity. The average orthogonal quality of the mesh is observed to be around 0.8.

LaDisa et al. [23] suggested that arterial walls with shear stress of less than 0.5 Pa would contribute to a higher risk of ISR formation as compared to arterial walls with shear stress of higher than 0.5 Pa. This is due to higher residence time and permeability of endothelial cells as compared to high WSS regions [24], which resulted in blood-borne particle uptake on the arterial wall [25]-[26].

In this study, the blood is set to be Newtonian fluid, turbulent and incompressible. Although recent studies stated that blood is non-Newtonian in its physiology, the blood can be assumed as Newtonian as the focus was on large arteries [2]. This is because the blood vessels can be considered bigger compared to the hematocytes as stated by Hegde et al. [17]. A study conducted by Liu et al. [27] found that the differences in WSS and pressure between Newtonian and non-Newtonian fluid models were small in both virtual and patient-specific models.

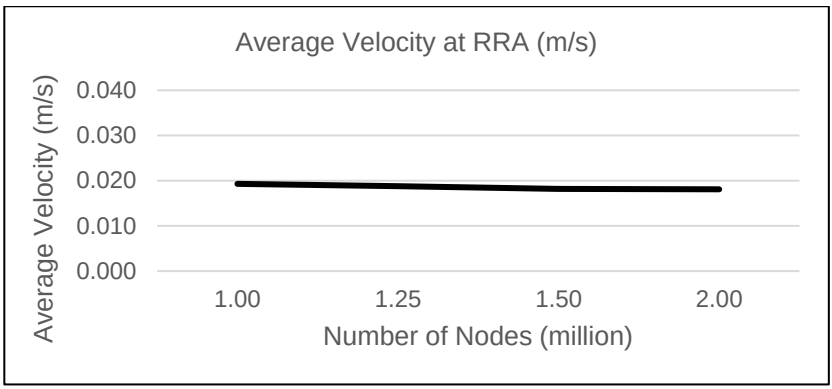

Figure 5: Grid independence test result for stented renal artery model

Results and Discussions

Flow characteristics

The average Reynolds number for flow at the abdominal aorta was found to be approximately 867, while at the renal artery, the Reynolds number is observed to be around 55 at the left renal artery and 73 at the right renal artery.

The recirculation region is observed at the proximal region of the renal artery, after the flow bifurcation region. The recirculation region indicates the occurrence of flow separation [28] after the bifurcation and reattachment of flow downstream of the renal artery. This is due to blood flow deceleration as the blood flow enters the renal artery, indicated by the low-velocity region near the wall [29]. The flow recirculation region especially after stent implantation is undesirable due to the increased residence time of the platelet, lipids, and white blood cells. This may lead to the formation of neointimal hyperplasia near the stent wall, thus increasing the risk of in-stent restenosis formation [30]-[31]. The flow characteristics are shown in Figure 6.

It is expected that the blood velocity for the stented renal artery model in this study should be close to the blood velocity of the normal renal artery.

Clinical measurements suggested that the normal blood velocity in a renal artery should range between 0.6 m/s and 1 m/s [32]-[33]. All stented renal artery models recorded blood flow velocity ranges between 0.65 m/s and 1.3 m/s which indicates that the simplified model used in this study is valid for the representation of the renal artery.

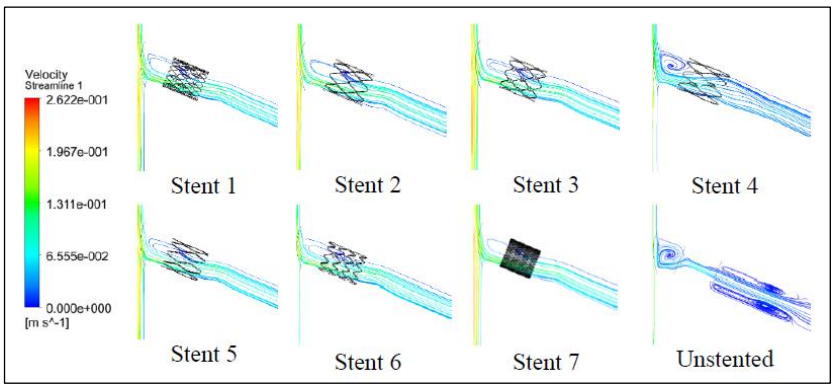

Figure 6: Flow behaviour in stented and unstented renal artery model

Analysing the flow behaviour alone does not clearly illustrate the effect of stent design on in-stent restenosis formation. This is due to the flow parameters, i.e. pressure, velocity, and flow direction, only partially representing the potential of restenosis formation on the arterial wall. Therefore, observing the behaviour of WSS on the arterial wall would be beneficial in this effort.

Wall shear stress

Wall shear stress visualization caused by blood flow on the arterial wall for stented and unstented renal arteries is shown in Figure 7. All stented arterial walls in this study showed a significant reduction in WSS as compared to unstented stenosed arteries. Unfortunately, all stent designs recorded low WSS of less than 0.5 Pa on most of its surface area. This is undesirable as the risk of blood-borne uptake at the arterial wall would increase due to flow stagnation [5]. The reason behind this phenomenon could be due to the occurrence of flow separation near the arterial wall caused by the separation of contact between the fluid and the arterial wall by the stent.

Figure 8 shows the comparison of the percentage of area with low WSS for all stent designs that were evaluated in this study. Stent 1 shows the lowest area percentage with low WSS at 94.32% which was 1.76% below the average area with low WSS across all stent designs. However, the area percentage was not significantly different from Stent 4 which has the highest area percentage

of low WSS area at 99.13%. The difference of 4.81% might not significantly contribute to the reduction in risk of in-stent restenosis formation for Stent 1 as compared to Stent 4.

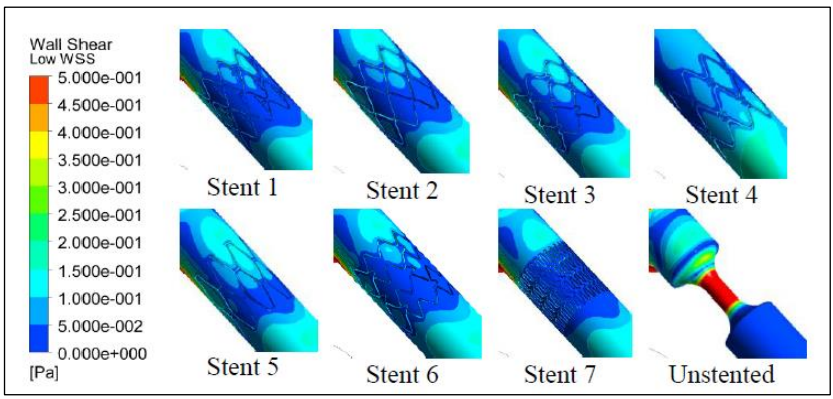

Figure 7: Wall shear stress on stented and unstented renal artery model

Although a small reduction in the area with low WSS by varying stents' design configuration, the results show promising effects of the design configuration on the reduction of the area with low WSS. This is believed worth to be further explored. The reduction of low WSS area on the renal arterial wall with Stent 1 could be due to the strut spacing closest to the optimum design at that point of study, which of course requires further improvement. This is supported by He et al. [34] study that suggests a larger longitudinal distance between struts' adjacent rows would increase WSS on the arterial wall.

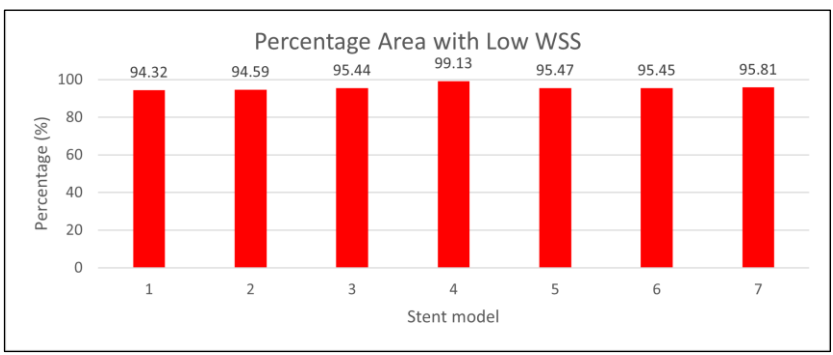

Figure 8: Comparison of arterial wall area with low WSS for stented renal artery

Stent thickness

Variation of stent thickness was performed on Stent 1, which was selected based on the results of the lowest area with low WSS, to evaluate the thickness effect on the flow behaviour. WSS behaviour for three thicknesses of Stent 1 (0.15 mm, 0.20 mm, and 0.25 mm) is shown in Figure 9. Although there was still a large area with low WSS on the stent, reduction of stent thickness has shown promising results in reducing surface area with low WSS. This is supported by the finding that thinner stent strut is associated with a lower risk of stent thrombosis or restenosis [35].

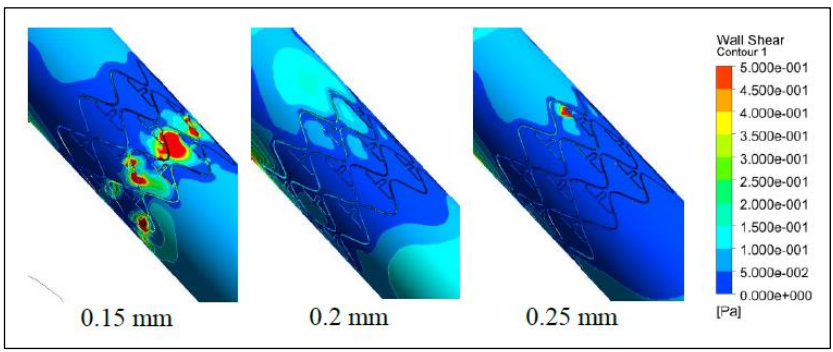

Figure 9: Low WSS area contour plot on renal artery wall for stents with different strut thickness of Stent 1

Table 2 shows the percentage of area exposed to low WSS due to different strut thickness. The strut thickness affects the percentage of area covered by low WSS. Stent 1 with 0.15 mm strut thickness recorded the lowest area with low WSS as compared to Stent 1 with 0.2 mm and 0.25 mm strut thickness. This suggests that decreasing the stent's strut thickness could potentially improve the WSS on the arterial wall hence reducing the risk of in-stent restenosis formation. Reducing the stent's strut thickness by 0.05 mm could potentially reduce the area with low WSS by about 3.3%. This directly indicates that less thickness of the stent's strut would contribute to the reduction of in-stent restenosis formation risk.

Table 2: Low WSS area percentage for three different strut thicknesses of Stent 1

Strut thickness (mm)	Low WSS area percentage
0.15	90.97%
0.20	94.32%
0.25	95.11%

Conclusion

The use of computational fluid dynamics to evaluate the contributing risk factors to in-stent restenosis formation for renal artery in this study had shown a promising method for that purpose. Out of the seven selected stent designs, Stent 1 showed promising results with the least low WSS area of 1.49% below the average low WSS area recorded in this study, contributed by its strut configurations. Next, by reducing the Stent 1 strut thickness to 0.15 mm, the low WSS area further dropped by 3.3%. However, as the reduction of low WSS area was not yet up to the significant value to be claimed effective in preventing in-stent restenosis occurrence, it is worth further pursuing the development of this study. This is due to the promising combination of results obtained in this study that shows possibilities of further positive findings.

Contributions of Authors

The authors confirm the equal contribution in each part of this work. All authors reviewed and approved the final version of this work.

Funding

The authors would like to acknowledge the financial support from Universiti Teknologi Malaysia for the funding under UTM Fundamental Research (UTMFR) (Q.J130000.2551.21H62).

Conflict of Interests

All authors declare that they have no conflicts of interest.

Acknowledgment

The authors would like to acknowledge the financial support from Universiti Teknologi Malaysia for the funding under UTM Fundamental Research (UTMFR) (Q.J130000.2551.21H62).

References

[1] L. Dobrek, "An Outline of Renal Artery Stenosis Pathophysiology—A Narrative Review", *Life*, vol. 11, no. 3, pp. 1-19, 2021.

[2] A. Khader, A. Azriff, C. Johny, R. Pai, M. Zuber, K. A. Ahmad, and Z. Ahmad, "Haemodynamics behaviour in normal and stenosed renal artery using computational fluid dynamics," *Journal of Advanced Research in Fluid Mechanics and Thermal Sciences*, vol. 51, no. 1, pp. 80-90, 2018.

[3] D. Wang, Y. Pan, X. Cai, J. Hing, H. Yan, S. Wang, W. Chan, L. Mei, Y. Zhang, S. Li, T. Wei, Y. L. Zhou, and Y. Wang "Prevalence and associated factors of atherosclerotic plaque and stenosis in renal arteries: A community-based study", *Angiology*, vol. 0, no. 0, p. 00033197241238404. 2024. doi: https://doi.org/10.1177/00033197241238404.

[4] M. Piechocki, T. Przewłocki, P. Pieniążek, M. Trystuła, J. Podolec, and A. Kabłak-Ziembicka, "A non-coronary, peripheral arterial atherosclerotic disease (carotid, renal, lower limb) in elderly patients—A review PART II—Pharmacological approach for management of elderly patients with peripheral atherosclerotic lesions outside coronary territory," *Journal of Clinical Medicine*, vol. 13, no. 5, pp. 1-45, 2024.

[5] J. Murphy and F. Boyle, "Predicting neointimal hyperplasia in stented arteries using time-dependant computational fluid dynamics: A review", *Computers in Biology and Medicine*, vol. 40, no. 4, pp. 408-418, 2010. doi: https://doi.org/10.1016/j.compbiomed.2010.02.005

[6] M. C. Jundt, E. A. Takahashi, W. S. Harmsen, and S. Misra, "Restenosis rates after drug-eluting stent treatment for stenotic small-diameter renal arteries", *Cardiovascular and Interventional Radiology*, vol. 42, no. 9, pp. 1293-1301, 2019.

[7] K. Zachrisson, S. Elverfors, G. Jensen, M. Hellstrom, M. Scensson, H. Herlitz, M. Falkenberg, "Long-term outcome of stenting for atherosclerotic renal artery stenosis and the effect of angiographic restenosis", *Acta Radiologica*, vol. 59, no. 12, pp. 1438-1445, 2018.

[8] R. Gharleghi, H. Wright, V. Luvio, N. Jepson, Z. Luo, A. Senthurnathan, B. Babaei, G. B. Prusty, T. Ray, and S. Beier, "A multi-objective optimization of stent geometries," *Journal of Biomechanics*, vol. 125, no. 1, pp. 1-11, 2021.

[9] B. Chezeau and C. Vial, "Modeling and Simulation of the Biohydrogen Production Processes," in *Biohydrogen*, 2nd Ed. Elsevier B. V., pp. 445-483, 2019.

[10] P. Wang, H. Qiao, R. Wang, R. Hou, and J. Guo, "The characteristics and risk factors of in-stent restenosis in patients with percutaneous coronary intervention: what can we do", *BMC Cardiovascular Disorders*, vol. 20, no. 1, pp. 1-6, 2020.

[11] M. A. Hamidah and S. M. C. Hossain, "Modeling analysis of pulsatile non-Newtonian blood flow in a renal bifurcated artery with stenosis," *International Journal of Thermofluids*, vol. 22, pp. 1-15, 2024.

[12] A. Mandaltsi, A. Grytsan, A. Odudu, J. Kadziela, P. D. Morris, A. Witkowski, T. Ellam, P. Kalra, and A. Marzo, "Non-invasive stenotic renal artery haemodynamics by in silico medicine", *Frontiers in Physiology*, vol. 9, pp. 1-10, 2018.

[13] X. Song, H. Qiu, S. Wang, Y. Cao, and J. Zhao, "Hemodynamic and geometric risk factors for in-stent restenosis in patients with intracranial atherosclerotic stenosis," *Oxidative Medicine and Cellular Longevity*, vol. 2024, pp. 1-15, 2022.

[14] S. F. Mohamad, M. S. Bin Shamsul Ismail, M. A. A.-F. Bin Mohd Raffali, D. Farouk, R. M. Ali, and H. H. Che Hassan, "TCTAP C-148 the masquerading pickering; in-stent restenosis of renal artery stenting with contralateral renal artery stenosis presenting with flash acute pulmonary edema," *Journal of the American College of Cardiology*, vol. 79, no. 15, Supplement, pp. 351-352, 2022.

[15] D. Stojadinovic, I. Zivanovic-Macuzic, M. Jakovcevski, D. Jeremic, M. Kovacevic, and M. Minic, "The anatomy of renal arteries in adults " *Journal of Experimental and Applied Biomedical Research (EABR)*, vol. 23, no. 2, pp. 147-153, 2022.

[16] I. Taib, M. R. A. Kadir, M. H. S. A. Azis, A. Z. Md Khudzari, and K. Osman, "Analysis of hemodynamic differences for stenting patent ductus arteriosus," *Journal of Medical Imaging and Health Informatics*, vol. 3, no. 4, pp. 555-560, 2013.

[17] P. Hegde, S. Kanjalkar, G. Shenoy, A. Khader, R. Pai, M. Tamahawa, R. Prabhu, and D. S. Rao, "Quantitative haemodynamic study in renal artery bifurcation using CFD," *Journal of Engineering Science and Technology*, vol. 16, no. 5, pp. 4079-4099, 2021.

[18] Y. Zhao, Y. Shi, Y. Jin, Y. Cao, H. Song, L. Chen, F. Li, X. Li, and W. Chen, "Evaluating short-term and long-term risks associated with renal artery stenosis position and severity: a hemodynamic study", *Bioengineering*, vol. 10, no. 9, pp. 1-13, 2023.

[19] B. M. Johnston, P. R. Johnston, S. Corney, and D. Kilpatrick, "Non-Newtonian blood flow in human right coronary arteries: steady state simulations," *Journal of Biomechanics*, vol. 37, no. 5, pp. 709-720, 2004.

[20] A. Ismail, B. L. Ademola, L. Yusuf, and M. A. Abdulmalik, "Renal arterial doppler velocimetric indices among healthy subjcts in north west nigeria," *West African Journal of Medicine*, vol. 8, no. 1, pp. 40-49, 2019.

[21] M. A. Kabir, M. F. Alam, and M. A. Uddin, "Numerical simulation of pulsatile blood flow: a study with normal artery, and arteries with single and multiple stenosis," *Journal of Engineering and Applied Science*, vol. 68, no. 1, pp. 1-15, 2021.

[22] S. S. Varghese and S. H. Frankel, "Numerical modeling of pulsatile turbulent flow in stenotic vessels," *Journal of Biomechanical Engineering*, vol. 125, no. 4, pp. 445-460, 2003.

[23] J. F. LaDisa, L. E. Olson, R. C. Molthen, D. Hettrick, P. Pratt, M. D> Hardel, J. Kersten, D. C. Warltier, P. S. Pagel, "Alterations in wall shear stress predict sites of neointimal hyperplasia after stent implantation in rabbit iliac arteries," *American Journal of Physiology-Heart and Circulatory Physiology*, vol. 288, no. 5, pp. 2465-2475, 2005.

[24] C. Trenti, M. Ziegler, N. Bjarnegård, T. Ebbers, M. Lindenberger, and P. Dyverfeldt, "Wall shear stress and relative residence time as potential risk factors for abdominal aortic aneurysms in males: A 4D flow cardiovascular magnetic resonance case–control study," *Journal of Cardiovascular Magnetic Resonance*, vol. 24, no. 1, pp. 1-12, 2022.

[25] G. B. Kim, K. H. Park, and S. J. Kim, "Hemodynamics and wall shear stress of blood vessels in aortic coarctation with computational fluid dynamics simulation", *Molecules*, vol. 27, no. 4, pp. 1-19, 2022.

[26] M. J. Gomez-Garcia, M. Abdelkarim, D. T. Cramb, S. J. Childs, K. D. Rinker, and H. I. Labouta, "Blood vessel wall shear stress determines regions of liposome accumulation in angiogenic vasculature", *Drug Delivery and Translational Research*, vol. 0, no. 0, pp.0 , 2024.

[27] H. Liu, L. Lan, J. Abrigo, H. L. Ip, Y. Soo, D. Zheng, K. S. L. Wong, D. Wang, L. Shi, T. W. Leung, X. Leng, "Comparison of newtonian and non-newtonian fluid models in blood flow simulation in patients with intracranial arterial stenosis", *Frontiers in Physiology*, vol. 12, no. 718540, pp. 1-11, 2021.

[28] A. G. Rahma and T. Abdelhamid, "Hemodynamic and fluid flow analysis of a cerebral aneurysm: a CFD simulation", *SN Applied Sciences*, vol. 5, no. 2, pp. 1-14, 2023.

[29] M. S. Hameed, A. A. Shah, M. I. Khan, A. Ali, I. Hussain, and M. D. Bukhari, "Comparison of blood flow analysis in stenosed and stented carotid artery bifurcation models", *Cogent Engineering*, vol. 10, no. 1, pp. 1-19, 2023.

[30] A. Javadzadegan, A. Yong, M. Chang, A. C. C. Ng, J. Yiannikas, M. K. C. Ng, M. Behnia, and L. Kritharides, "Flow recirculation zone length and shear rate are differentially affected by stenosis severity in human coronary arteries", *AJP Heart and Circulatory Physiology*, vol. 304, no. 4, pp. 559-566, 2013.

[31] G.-B. Kim, K.-H. Park, and S.-J. Kim, "Hemodynamics and wall shear stress of blood vessels in aortic coarctation with computational fluid dynamics simulation", *Molecules*, vol. 27, no. 4, pp. 1-19, 2022.

[32] B. K. Park, "Gray-scale, color doppler, spectral doppler, and contrast-enhanced renal artery ultrasound: imaging techniques and features," *Journal of Clinical Medicine*, vol. 11, no. 14, pp. 1-12, 2022.

[33] S. Al-Katib, M. Shetty, S. M. A. Jafri, and S. Z. H. Jafri, "Radiologic assessment of native renal vasculature: A multimodality review", *RadioGraphics*, vol. 37, no. 1, pp. 136-156, 2017.

[34] Y. He, N. Duraiswamy, A. O. Frank, and J. E. Moore, "Blood flow in stented arteries: a parametric comparison of strut design patterns in three dimensions," *Journal of Biomechanical Engineering*, vol. 127, no. 4, pp. 637-47, 2005.

[35] A. Saito, Z. Dai, M. Ono, T. Kanie, Y. Takaoka, A. Mizuno, N. Komiyama, and T. Asano, "The relationship between coronary stent strut thickness and the incidences of clinical outcomes after drug-eluting stent implantation: A systematic review and meta-regression analysis", *Catheterization and Cardiovascular Interventions*, vol. 99, no. 3, pp. 575-582, 2022.